ISIJ International, Vol. 63 (2023), No. 8, pp. 1394–1404
https://doi.org/10.2355/isijinternational.ISIJINT-2023-103

Electrodeposition Behavior of Zn–Ni Alloy from Alkaline Zincate Solutions Containing Various Brighteners and its Microstructure

Wataru MURAKAMI,[1)] Satoshi OUE,[2)] Yu-ki TANINOUCHI,[2)] Shinya AKAMATSU[3)] and Hiroaki NAKANO[2)]*

1) Graduate School of Engineering, Kyushu, University. Now at Mitsui Mining & Smelting, Co., Ltd., 1333-2 Haraichi, Ageo-shi, Saitama, 362-0021 Japan.
2) Faculty of Engineering, Kyushu University, 744, Motooka, Nishi-ku, Fukuoka-shi, 819-0395 Japan.
3) Yuken Industry Co., Ltd., 50, Bawari, Noda, Kariya-shi, 448-8511 Japan.

(*Received on March 31, 2023; accepted on April 20, 2023; originally published in Tetsu-to-Hagané, Vol. 109, 2023, No. 4, pp. 277–288*)

The effect of brighteners on the deposition behavior of Zn–Ni alloys and their microstructure was investigated. Zn–Ni alloys were electrodeposited on Cu electrode at 10–5 000 $A \cdot m^{-2}$, 10^5 $C \cdot m^{-2}$, and 308 K. Although the degree of suppression of hydrogen evolution differed depending on the kind of brightener, the transition current density at which the deposition behavior shifted from normal to anomalous was practically the same in all the solutions containing brighteners. The current efficiency of the alloy deposition significantly decreased with the addition of brighteners, which had a suppression effect on the Zn deposition. Considering that the brighteners suppressed the Ni deposition more than the Zn deposition, the Ni content in the deposited films decreased with the addition of brighteners. When the brightener of a straight-chain polymer comprising a quaternary ammonium cation (PQ) that can suppress the diffusion of ZnO_2^{2-} and Ni ions in a solution was added, the Ni content in the deposited films increased with increasing current density in a high-current-density region. This was attributed to the fact that Zn, which was preferentially deposited over Ni earlier, reached the diffusion limitation of ZnO_2^{2-}, and Ni deposition did not reach the diffusion-limited current density. When PQ and a quaternary ammonium salt with a benzene ring were added to the solution, the films obtained at the diffusion-limited current density of ZnO_2^{2-} exhibited smooth surfaces comprising fine crystals. With the addition of brighteners to increase the overpotential for deposition, the γ-phase (the intermetallic compound of Ni_2Zn_{11}) of the deposited films easily formed.

KEY WORDS: zincate; zinc-nickel alloy; electrodeposition; brightener; anomalous codeposition; polarization curve; current density; transition current; current efficiency; diffusion.

1. Introduction

Zn–Ni alloy electroplated steel sheets have been widely used in the production of automobile engine parts, home electrical appliances, and building materials because of their excellent corrosion resistance.[1–7)] Zn–Ni alloy electrodeposition is generally performed using sulfate and chloride solutions; however, zincate solution is known to be superior because of its throwing power during electrodeposition.[8,9)] The deposition of the Zn–Ni alloy from sulfate and chloride solutions has been extensively studied, and the anomalous codeposition behavior where the electrochemically less noble Zn was preferentially deposited over the nobler Ni has been observed in a practical current-density region.[10–14)]

Conversely, Zn–Ni alloy deposition from zincate solution has been reported to exhibit normal and anomalous behaviors depending on the deposition conditions,[15–20)] but these studies are few, compared with those using sulfate and chloride solutions. During deposition from a zincate solution, the brightener is generally added to the solution, but the effect of brighteners on the deposition behavior remains unclear. Therefore, we previously investigated the Zn–Ni alloy deposition behavior from a solution containing the reaction product of epichlorohydrin and imidazole (IME) as a brightener and reported that IME decreased the transition current density at which the deposition behavior shifted from normal to anomalous and decreased the Ni content in the deposits and the current efficiency of the alloy deposition.[21–26)] However, the effect of brighteners is unknown in a high-current-density region where the Zn–Ni alloy deposition proceeds under the diffusion control of ions. IME suppresses the charge-transfer process of deposition; however, a brightener that suppresses the diffusion of ions in solution is reported.[27–30)]

* Corresponding author: E-mail: nakano@zaiko.kyushu-u.ac.jp

Herein, a straight-chain polymer comprising a quaternary ammonium cation (PQ) is reported to suppress the diffusion of ZnO_2^{2-} during pure Zn deposition from zincate solution. When a quaternary ammonium salt with a benzene ring (QA) coexists with PQ, the suppression effect of the diffusion of ZnO_2^{2-} is reported to further increase.[27–30] Therefore, in addition to IME, we selected PQ, and QA, which are reported to suppress the diffusion of ZnO_2^{2-} as a brightener of pure Zn deposition from a zincate solution. We discuss the effect of brighteners on the Zn−Ni alloy deposition behavior in a wide current-density range of 10–5 000 $A \cdot m^{-2}$ based on the partial polarization curves for Zn and Ni depositions and hydrogen evolution.

2. Experimental Process

Table 1 shows the composition of the zincate solution and the electrolysis conditions. The electrolyte solutions were prepared by dissolving reagent-grade ZnO (0.15 $mol \cdot dm^{-3}$), $NiSO_4 \cdot 6H_2O$ (0.016 $mol \cdot dm^{-3}$), $N(CH_2CH_2OH)_3$ (0.34 $mol \cdot dm^{-3}$), and NaOH (2.5 $mol \cdot dm^{-3}$) in distilled and deionized water at room temperature. The brighteners listed in **Table 2** were added to this solution. Quaternary ammonium salt with a benzene ring (QA), a straight-chain polymer comprising a quaternary ammonium cation (molecule length: 20 nm, PQ) and a reaction product of epichlorohydrin and imidazole (IME) were added to the electrolyte solution at concentrations of 0.07, 1.45 $g \cdot dm^{-3}$, and 3 $mL \cdot dm^{-3}$, respectively. PQ is an inhibitor of diffusion of ZnO_2^{2-}, and QA is an auxiliary material of PQ. IME was added as an inhibitor of charge transfer for deposition. IME was prepared as previously reported.[31,32]

Electrolysis was performed using the constant-current electrolysis method without stirring at a current density in the range of 10–5 000 $A \cdot m^{-2}$, an amount of electricity of 10^5 $C \cdot m^{-2}$, and a solution temperature of 303 K. The amount of electricity of 10^5 $C \cdot m^{-2}$ corresponds to a film thickness of 4.7 μm, assuming the deposition of pure Zn at a current efficiency of 100%. A Cu plate (1 × 2 cm) was used as the cathode, and a Pt plate (1 × 2 cm) was used as the anode. However, when preparing samples for scanning electron microscopy (SEM) and X-ray diffraction (XRD), a Fe plate (1 × 2 cm) was used as the cathode. The deposited films were dissolved in nitric acid, and Zn and Ni were determined by inductively coupled plasma optical emission spectroscopy (ICP-OES) to obtain the composition of the deposited alloy and the current efficiencies of the Zn and Ni depositions. The current efficiency of the hydrogen evolution was determined by subtracting the current efficiencies (%) of the Zn and Ni depositions from 100. The partial current densities for the Zn and Ni depositions and hydrogen evolution were calculated by multiplying the total current density by the respective current efficiencies (%)/100. An Ag/AgCl electrode (saturated KCl, 0.199 V vs. normal hydrogen electrode (NHE), 298 K) was used as a reference electrode to measure the polarization curves, but the potentials were converted into the standard hydrogen electrode.

The surface morphology of the deposited films was observed by SEM, and the phase identification was performed using an X-ray diffractometer (Cu–Kα; tube voltage, 40 kV; tube current, 15 mA).

3. Results

3.1. Effect of Brighteners on the Deposition Behavior of Zn–Ni Alloys

Figure 1 shows the total polarization curve for the Zn–Ni alloy deposition. The equilibrium potential, E_{Zn}^{eq}, of the Zn deposition ($ZnO_2^{2-} + 2H_2O + 2e^- \rightarrow Zn + 4OH^-$), assuming that pure Zn was deposited at a solution temperature of 298 K, was −1.27 V.[33] In addition, the equilibrium potential, E_{Ni}^{eq}, of the Ni deposition ($Ni(TEA)_2^{2+} + 2e^- \rightarrow Ni + 2TEA$) was −0.41 V, based on the complex stabilization constant K = $10^{4.74}$ of triethanolamine (TEA) coordinated to Ni^{2+}, assuming that pure Ni was deposited at a solution temperature of 298 K.[34] The total polarization curve rose at a potential nobler than E_{Zn}^{eq} (−1.27 V), regardless of the presence of a brightener, and significantly shifted to a less noble potential region above a current density in the range of 20–50 $A \cdot m^{-2}$. When the potential reached E_{Zn}^{eq}, the total polarization curve rose again. The current density at which the cathode potential significantly shifted to a less noble

Table 1. Solution compositions and electrolysis conditions.

ZnO	($mol \cdot dm^{-3}$)	0.15	Current density ($A \cdot m^{-2}$)	10–5 000
$NiSO_4 \cdot 6H_2O$	($mol \cdot dm^{-3}$)	0.016	Temperature (K)	308
$N(CH_2CH_2OH)_3$	($mol \cdot dm^{-3}$)	0.34	Amount of charge ($C \cdot m^{-2}$)	10^5
NaOH	($mol \cdot dm^{-3}$)	2.5	Cathode	Cu or Fe (1×2 cm^2)
Brightener	($ml \cdot dm^{-3}$)	0–4.5	Anode	Pt (1×2 cm^2)
			Quiescent bath	

Table 2. Details of brighteners used in this study.

Symbol	Chemical agents	Suppression effect	Amount of addition
QA	Quaternary ammonium salt with a benzene ring	Adjuvant for PQ	0.07 ($g \cdot dm^{-3}$)
PQ	Straight-chain polymers composed of quaternary ammonium cation	Diffusion of ions in solution	1.45 ($g \cdot dm^{-3}$)
PQ+QA	—	Diffusion of ions in solution	1.45+0.07 ($g \cdot dm^{-3}$)
IME	Reaction product of epichlorohydrin and imidazole	Charge transfer of deposition	3.0 ($ml \cdot dm^{-3}$)

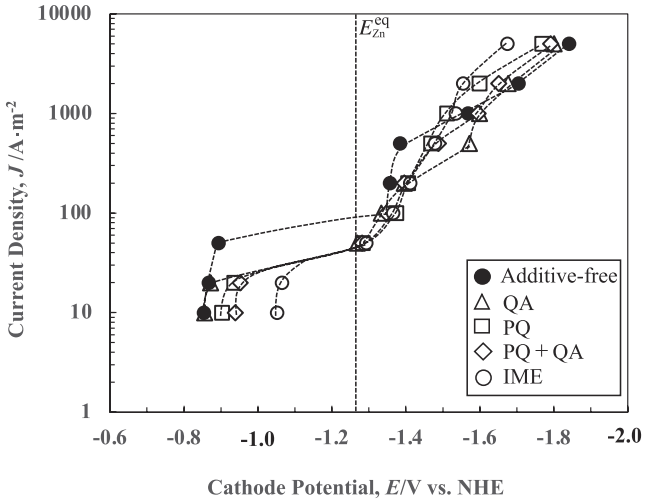

Fig. 1. Total polarization curves of the Zn–Ni alloy deposition from solutions containing various brighteners.

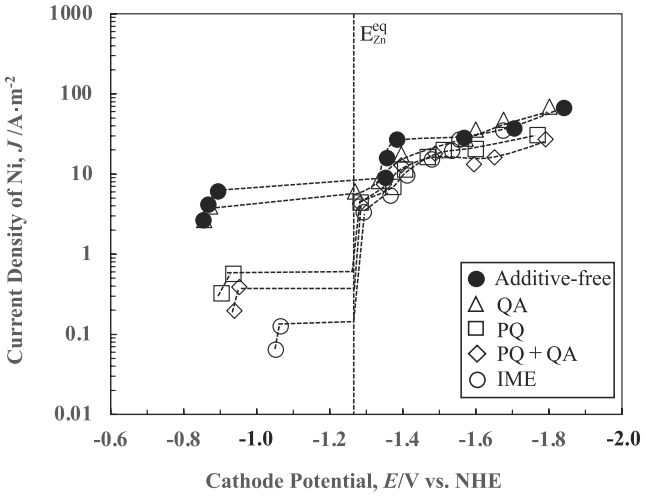

Fig. 3. Partial polarization curves of Ni during Zn–Ni alloy deposition from solutions containing various brighteners.

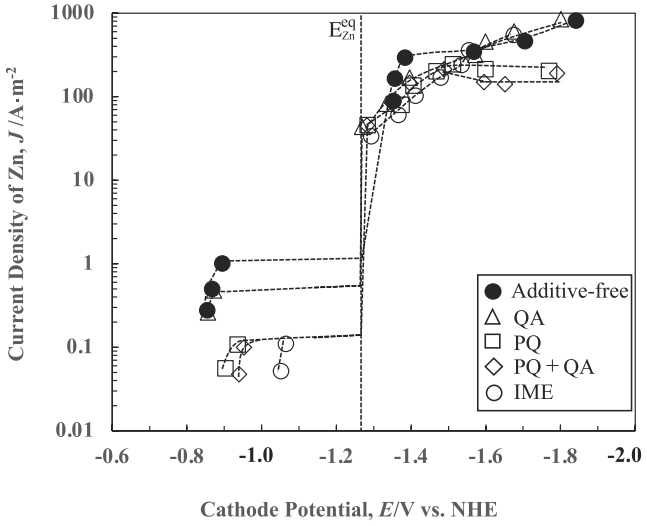

Fig. 2. Partial polarization curves of Zn during Zn–Ni alloy deposition from solutions containing various brighteners.

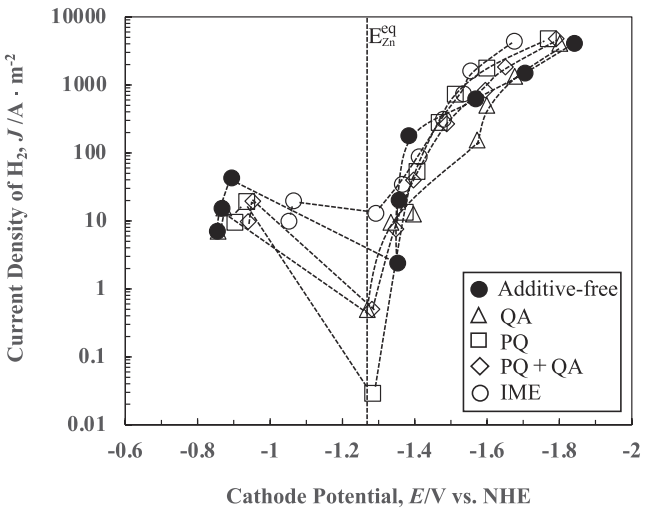

Fig. 4. Partial polarization curves of H_2 during Zn–Ni alloy deposition from solutions containing various brighteners.

potential was approximately 50 $A \cdot m^{-2}$ in a brightener-free solution, whereas it decreased to approximately 20 $A \cdot m^{-2}$ in brightener solutions regardless of the kind of brightener.

Regarding the difference in the brightener effect, at a potential region nobler than E_{Zn}^{eq}, the polarization was the highest with IME, and the polarization followed the order of (PQ + QA) > (PQ). Polarization was hardly observed with QA. Oppositely, in a potential region less noble than E_{Zn}^{eq}, the effect of the brightener differed depending on the current density. In the current-density region of 200–500 $A \cdot m^{-2}$, the cathode potential was polarized with the brightener, whereas it was depolarized with all the brighteners at a high current density above 2 000 $A \cdot m^{-2}$.

Figure 2 shows the partial polarization curve of Zn deposition during the Zn–Ni alloy deposition. The partial current density of Zn was detected even at a potential nobler than E_{Zn}^{eq} (−1.27 V), and the current density was relatively high without additives and with QA. At a potential less noble than E_{Zn}^{eq}, Zn deposition was suppressed with brighteners, regardless of the kind, in the Zn partial current-density range of 100–300 $A \cdot m^{-2}$. With PQ, the diffusion-limiting current density for Zn deposition was observed, and the diffusion-limiting current density decreased with the coexistence of QA. At a high Zn partial current density above 300 $A \cdot m^{-2}$, the suppression effect of IME and QA on Zn deposition was hardly observed.

Figure 3 shows the partial polarization curve of Ni deposition during the Zn–Ni alloy deposition. At a potential nobler than E_{Zn}^{eq} (−1.27 V), Ni deposition was suppressed the most with IME, and the suppression effect followed the order of (PQ + QA) > (PQ). The suppression effect of QA was hardly observed at a Ni partial current density below 4 $A \cdot m^{-2}$, whereas it was observed at a current density above 4 $A \cdot m^{-2}$. Oppositely, at a potential less noble than E_{Zn}^{eq}, the Ni deposition was suppressed with brighteners regardless of its kind, at a Ni partial current density above 10 $A \cdot m^{-2}$. In particular, with the addition of PQ and PQ + QA, the partial current density of Ni decreased owing to the diffusion control of Ni ions, but it did not reach the diffusion-limiting current density of the Ni ions, which differed from that of the Zn deposition.

Figure 4 shows the partial polarization curve for hydrogen evolution during the Zn–Ni alloy deposition. Hydrogen evolution from the Zn–Ni alloy solution once decreased

with a shift in the potential to a less noble direction regardless of the presence of a brightener at a potential nobler than E_{Zn}^{eq} and began to increase at a potential less noble than E_{Zn}^{eq}. Regarding the effect of brighteners on hydrogen evolution, at a potential nobler than E_{Zn}^{eq}, the potential for hydrogen evolution at the same current density of 10 A·m^{-2} shifted to a less noble direction with the addition of a brightener. The potential for hydrogen evolution mostly shifted to a less noble direction with IME, and the degree of the shift followed the order of (PQ + QA) > (PQ), which was identical to the effect on the Zn and Ni depositions. Conversely, at a potential less noble than E_{Zn}^{eq}, the hydrogen evolution was suppressed with the brightener at a hydrogen partial current density in the range of 10–200 A·m^{-2}, and the suppression effect of QA was particularly high. However, when the partial current density of hydrogen exceeded 1 000 A·m^{-2}, the suppression effect of the brightener on the hydrogen evolution disappeared, and conversely, its promotion effect was observed.

Figure 5 shows the relationship between the current density and current efficiency of Zn–Ni, Zn, and Ni depositions during the Zn–Ni alloy deposition. The current efficiency of the Zn–Ni alloy deposition shown below is the sum of the current efficiencies of the Zn and Ni depositions. In the brightener-free solution, the current efficiency of the Zn–Ni alloy deposition (Fig. 5(a)) was low (15%–30%) in the low-current-density range of 10–50 A·m^{-2} (a potential region nobler than E_{Zn}^{eq}). However, it rapidly increased above 50 A·m^{-2} and became maximum at 100 A·m^{-2} (the region of the rate-determining process of charge-transfer at a potential less noble than E_{Zn}^{eq}). Thereafter, the current efficiency decreased as the current density increased above 500 A·m^{-2} (the region of the rate-determining process of ion diffusion at a potential less noble than E_{Zn}^{eq}). Contrarily, with the addition of brighteners, the current efficiency significantly increased at a current density above 20 A·m^{-2} regardless of the kind of brightener and became maximum at 50 A·m^{-2}; thereafter, it decreased with increasing current density. The current density to drastically increase the current efficiency of the alloy deposition decreased with the addition of brighteners.

Regarding the difference in the effect of brighteners, at a low current density of 10–20 A·m^{-2} (a potential region nobler than E_{Zn}^{eq}), IME, and PQ decreased the current efficiency to approximately zero. However, QA hardly decreased the current efficiency. In the middle-current-density range of 50–500 A·m^{-2} (the region of the rate-determining process of charge transfer at a potential less noble than E_{Zn}^{eq}), IME decreased the current efficiency the most, followed by PQ. At a high current density above 1 000 A·m^{-2} (the region of the rate-determining process of ion diffusion at a potential less noble than E_{Zn}^{eq}), PQ + QA decreased the current efficiency the most, followed by PQ. QA slightly increased the current efficiency, compared with the brightener-free solution, at a current density above 200 A·m^{-2}.

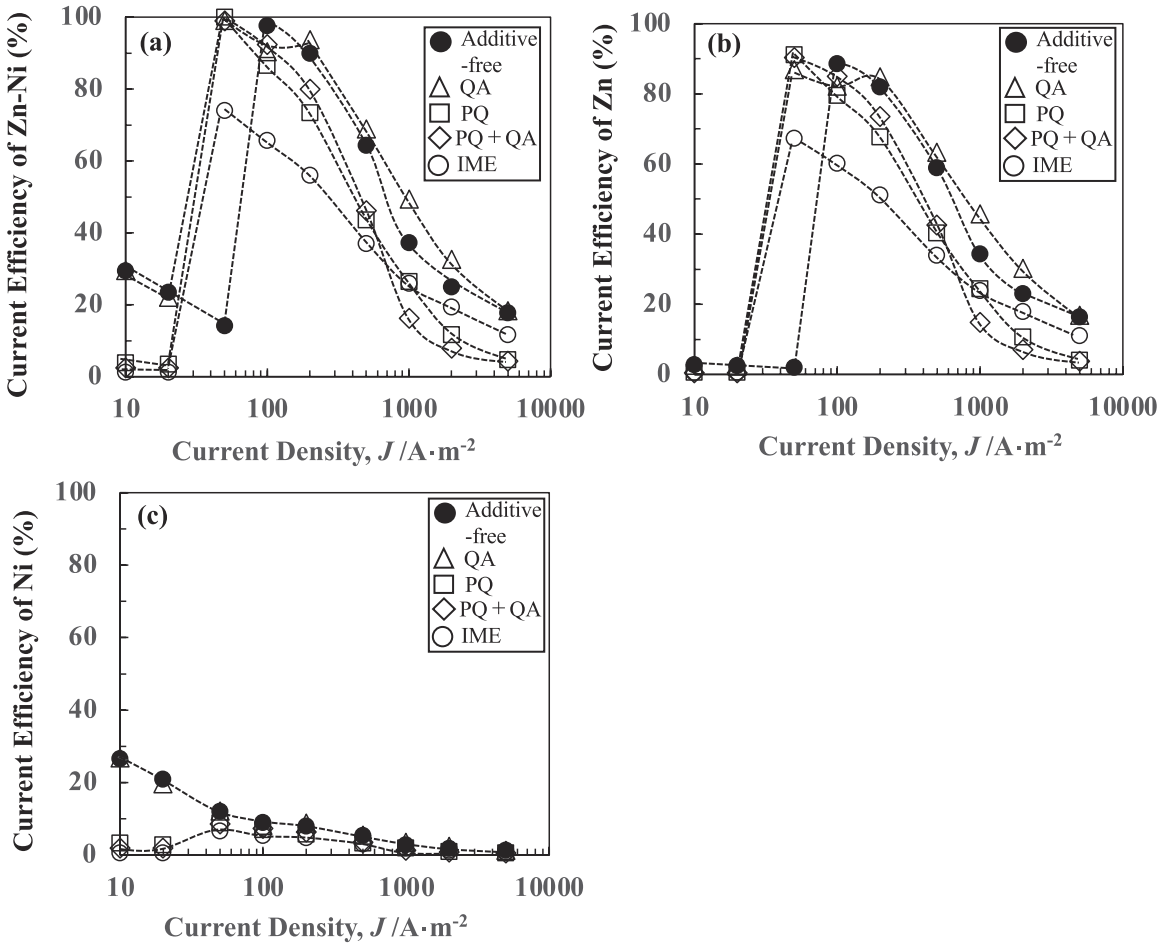

Fig. 5. Current efficiencies of the Zn–Ni alloy deposition from solutions containing various brighteners. (a) Zn–Ni, (b) Zn, (c) Ni.

The current efficiency of Zn deposition during the alloy deposition (Fig. 5(b)) was extremely low within a low-current-density range of 10–50 A·m^{-2} in the brightener-free solution and 10–20 A·m^{-2} in the brightener solutions but significantly increased as the current density exceeded 50 and 20 A·m^{-2}, respectively. The effect of brighteners on the current efficiency of Zn deposition at a current density above 50 A·m^{-2} was identical to that on the current efficiency of the aforementioned Zn−Ni alloy deposition. The effect of brighteners on the current efficiency of the Ni deposition during the alloy deposition (Fig. 5(c)) was observed within the low-current-density range of 10–20 A·m^{-2}; IME and PQ decreased the current efficiency of Ni to approximately zero. Comparing Figs. 5(a), 5(b), and 5(c), regardless of the presence of a brightener, the current efficiency of the Zn−Ni alloy deposition reflected the current efficiency of Ni in a low-current-density region (a potential nobler than E_{Zn}^{eq}) and the current efficiency of Zn in a middle-current-density region (the region of the rate-determining process of charge transfer at a potential less noble than E_{Zn}^{eq}) and high-current-density region (the region of the rate-determining process of ion diffusion at a potential less noble than E_{Zn}^{eq}), respectively. IME and PQ affected the current efficiency of the Ni deposition in a low-current-density region and the current efficiency of Zn in middle- and high-current-density regions, respectively.

Figure 6 shows the effect of current density on the Ni content of the Zn–Ni alloy deposited films. The broken line in the figure shows the composition reference line (CRL) of Ni, indicating that the Ni content in the solution was identical to that in the deposited films. When the Ni content in the deposited films exceeded the CRL, normal codeposition occurred, in which electrochemically nobler Ni was deposited in preference to Zn. Contrarily, when the Ni content in the deposited films was below the CRL, anomalous codeposition occurred, in which less noble Zn was deposited in preference to Ni. As shown in Fig. 6(a), in the brightener-free solution, the Ni content in the deposited films significantly changed in the current-density range of 50–100 A·m^{-2}. Below 50 A·m^{-2}, the Ni content was above the CRL at approximately 90 mass%, indicating normal-type codeposition, whereas, above 100 A·m^{-2}, it was below the CRL, indicating anomalous codeposition. The deposition behavior shifted from normal to anomalous at a certain current density called the transition current density.[35–37] With the addition of brighteners regardless of the kind, the Ni content in the deposited films significantly changed in the current-density range of 20–50 A·m^{-2} and became less than the CRL above 100 A·m^{-2}, indicating anomalous codeposition. Thus, the transition current density decreased with the addition of brighteners regardless of the kind. This transition current density correlated with the current density where the potential of the total polarization curve shown in Fig. 1 abruptly shifted from the region nobler than E_{Zn}^{eq} to a less noble region and the current density where the current efficiency of the Zn–Ni alloy deposition significantly changed (Fig. 5). Regarding the difference in the brightener effect, in the low-current-density range of 10–20 A·m^{-2}, IME decreased the Ni content of the deposited films the most, and the degree of the decrease in Ni content followed the order of (PQ+QA) > (PQ), and QA hardly affected the Ni content.

The enlarged images of the Ni content in the current-density region where anomalous codeposition occurred are shown in Fig. 6(b). Within the current-density range of 50–500 A·m^{-2}, the brightener slightly decreased the Ni content of the deposited films. However, the characteristic behavior of the Ni content of the deposited films increasing with increasing current density above 1 000 A·m^{-2} was observed in solutions containing PQ and PQ + QA.

3.2. Effect of Brighteners on the Appearance and Microstructure of the Deposited Films

Figure 7 shows the appearance of the Zn–Ni alloy deposition films obtained at 200 and 500 A·m^{-2}. In certain samples, the word that was written on a card placed opposite the sample was reflected on the sample during photographing. Thus, the clearer the word, the better the gloss of the deposited films. In the brightener-free solution, the deposited films were gray and matte at any current density. With the addition of QA, the appearance was virtually identical in the brightener-free solution, whereas it became glossy at

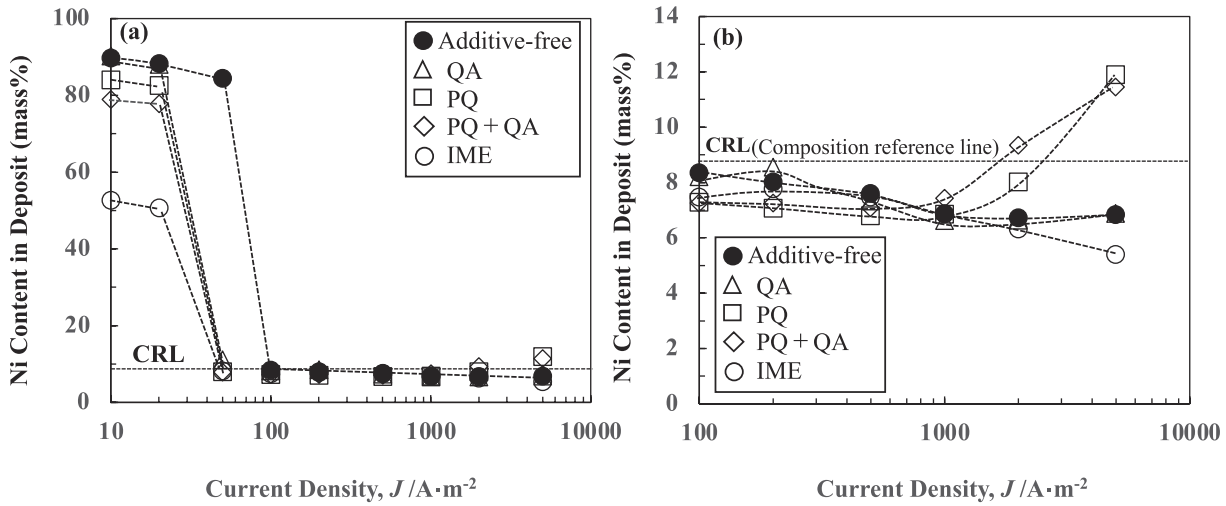

Fig. 6. (a) Ni contents in the Zn–Ni alloys deposited from the solutions containing various brighteners. (b) Magnified view of the area of 0–14 mass% of the Ni content.

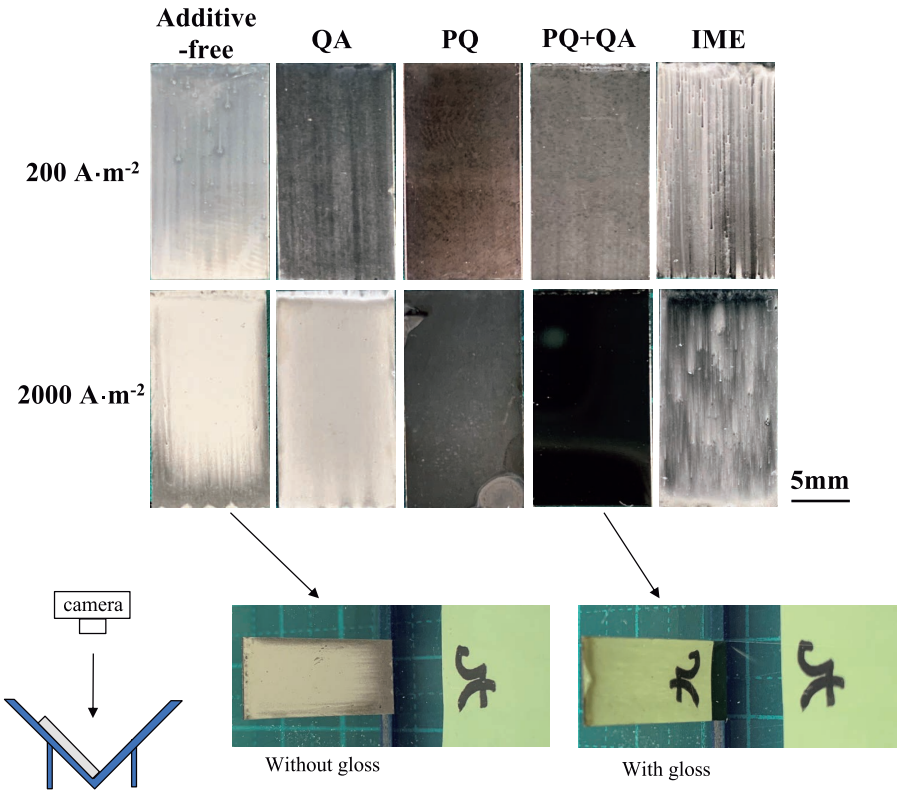

Fig. 7. Appearance of Zn–Ni alloy films deposited from the solutions containing various brighteners. (Online version in color.)

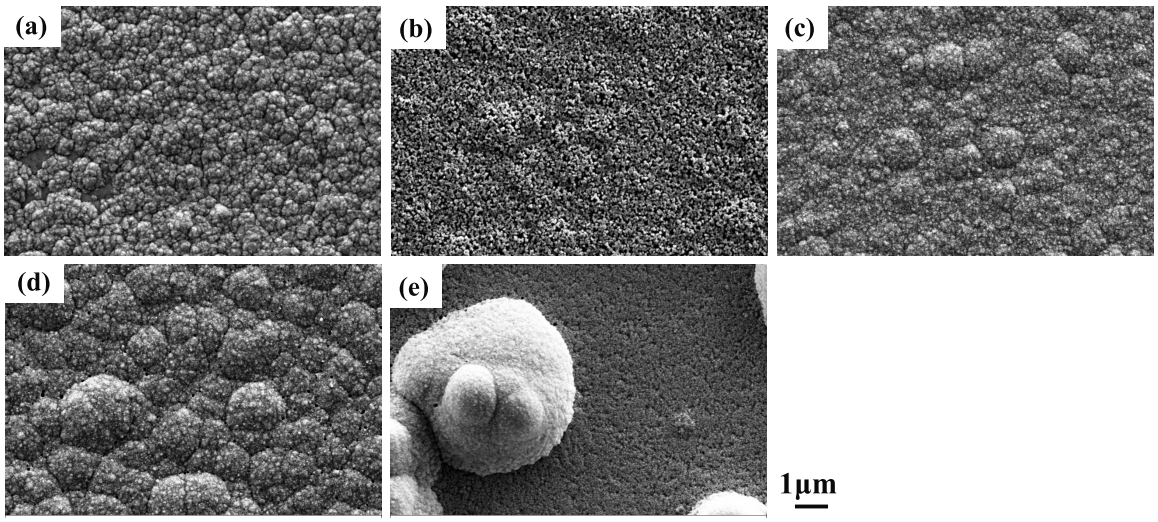

Fig. 8. SEM images of the Zn–Ni alloy films deposited at 200 A·m^{-2} from the (a) brightener-free, (b) QA, (c) PQ, (d) PQ + QA, and (e) IME solutions.

2 000 A·m^{-2} with PQ, and the gloss further increased with PQ + QA.

Figure 8 shows the SEM images of the films deposited at the middle current density of 200 A·m^{-2} (the region of the rate-determining process of charge transfer at a potential less noble than E_{Zn}^{eq}). Here, 200 A·m^{-2} was located in the anomalous codeposition region. The Ni content of the deposited films was in the range of 7.1–8.6 mass%, regardless of the presence or kind of brightener, and the difference in the Ni content between samples was small (Fig. 6(b)). The film deposited from the brightener-free solution comprised granular crystals with a size of approximately 0.2 μm (Fig. 8(a)). QA (b), PQ (c), and PQ + QA (d) decreased the crystal size, compared with the films deposited from the brightener-free solution (a). In particular, QA (b) significantly decreased the crystal size. With the addition of IME (e), large granular crystals with a size of several micrometers were observed on smooth crystals. The large granular crystals appeared to be aggregations comprising fine crystals.

Figure 9 shows the XRD patterns of the films (Ni content, 7.1–8.6 mass%) deposited at 200 A·m^{-2}. The brightener-free solution (a) exhibited a major peak from the η-Zn phase, and weak peaks related to the γ-phase (the intermetallic compound of Ni_2Zn_{11}) were observed. With QA (b), the XRD pattern showed the same trend as that

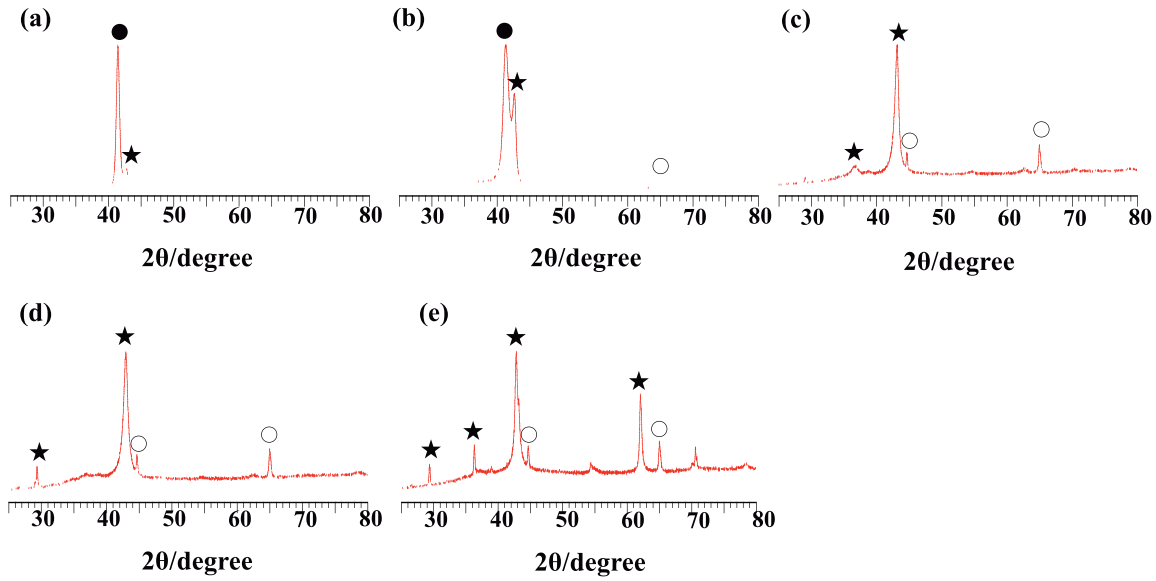

Fig. 9. X-ray diffraction patterns of the Zn–Ni alloy films deposited at 200 A·m^{-2} from the (a) brightener-free, (b) QA, (c) PQ, (d) PQ + QA, and (e) IME solutions. (○ Fe PDF # 65-4899, ● Zn[η] PDF # 87-0713, and ★ Ni_2Zn_{11}[γ] PDF # 65-5310) (Online version in color.)

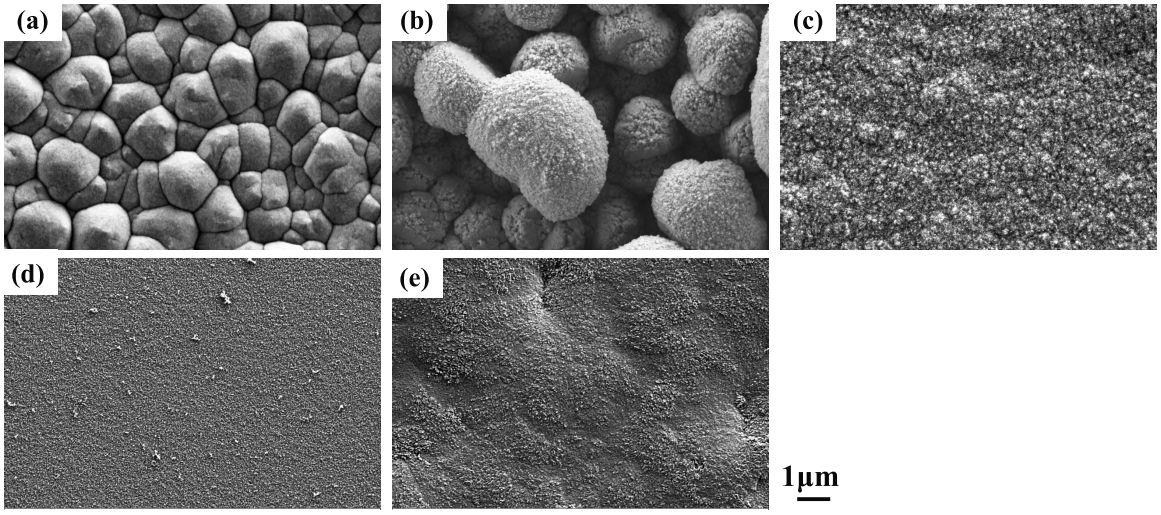

Fig. 10. SEM images of the Zn–Ni alloy films deposited at 2 000 A·m^{-2} from the (a) brightener-free, (b) QA, (c) PQ, (d) PQ + QA, and (e) IME solutions.

of the brightener-free solution, but the γ-phase peak was stronger than that of the brightener-free solution. With PQ (c), only the γ-phase peaks were observed along with the peaks of the Fe substrate; the peak of the η-Zn phase was not observed. With PQ + QA (d) and IME (e), the XRD patterns showed almost the same trend as that with PQ (c). The Ni contents of the deposited films were 8.0 and 8.6 mass% in the brightener-free and QA-added solutions, respectively, whereas they were 7.1, 7.3, and 7.8 mass% with PQ, PQ + QA, and IME, respectively. Although the Ni contents of the deposited films decreased with PQ, PQ + QA, and IME, only the γ-phase was formed.

Figure 10 shows the SEM images of the films deposited at a high current density of 2 000 A·m^{-2} (the region of the rate-determining process of ion diffusion at a potential less noble than E_{Zn}^{eq}). The Ni contents of the films deposited at 2 000 A·m^{-2} were in the range of 6.3–9.3 mass% (Fig. 6(b)). The film deposited in the brightener-free solution comprised granular crystals with a size of approximately 1 μm (Fig. 10(a)). QA (b) increased the crystal size, but PQ (c) decreased the size, and PQ + QA (d) further decreased the size, resulting in a smooth surface. IME (e) decreased the crystal size but produced slight roughness. The crystal size of the films deposited from the brightener-free solution was approximately 1 μm at the high current density of 2 000 A·m^{-2} (Fig. 10(a)), whereas it was approximately 0.2 μm at the middle current density of 200 A·m^{-2} (Fig. 8(a)), indicating that the crystal size increased with an increase in current density. Generally, the nucleation of crystals prevails over growth with increasing current density, resulting in a decrease in the crystal size. However, the opposite tendency was observed in the present study. During Zn deposition, it is reported that the current concentrates on the salient area of deposits under the rate-determining condition of Zn^{2+} diffusion, and the crystal size increases.[38] Here, Zn and Ni were deposited during the rate-determining step of the

ZnO_2^{2-} diffusion and Ni ions at 2 000 A·m^{-2} (Figs. 1–3), which appeared to increase the crystal size.

Figure 11 shows the XRD patterns of the films (Ni content, 6.3–9.3 mass%) deposited at 2 000 A·m^{-2}. The brightener-free solution (a) exhibited a major peak from the η-Zn phase, and the peaks related to the γ-phase (the intermetallic compound of Ni_2Zn_{11}) were faintly detected. With QA (b), the γ-phase peaks were mainly observed along with the η-Zn phase peak. With PQ (c), γ-phase peaks were mainly detected; the η-Zn phase peak was faintly observed. However, only the γ-phase peaks were detected along with the peaks of the Fe substrate with PQ + QA (d); the η-Zn phase peak was not observed. With IME (e), the γ-phase peaks were mainly detected along with the η-Zn phase peak. The Ni content of the deposited films was 6.7 mass% without brighteners, whereas they were 6.6, 8.0, 9.3, and 6.3 mass% with QA, PQ, PQ + QA, and IME, respectively.

Figures 9 and 11 show that the films deposited at 200 and 2 000 A·m^{-2} mainly comprised the η-Zn phase without brighteners, but they mainly comprised the γ-phase with PQ, PQ + QA, and IME. With QA, the γ-phase was more predominant at 2 000 A·m^{-2} than at 200 A·m^{-2}. The effect of current density on the formation of the γ-phase was hardly observed without and with brighteners, except for QA.

4. Discussion

The effect of brighteners on the deposition behavior of Zn–Ni alloys from alkaline zincate solutions and their morphology is summarized in **Table 3**. With PQ, the diffusion-limiting current density for Zn deposition was observed, and it decreased with the coexistence of QA (Fig. 2). With PQ and PQ + QA, the region where the partial current density of Ni decreased owing to the rate-determining process of Ni-ion diffusion was observed (Fig. 3). Thus, the brightener, PQ, used in this study had a suppression effect on the diffusion of ZnO_2^{2-} and Ni ions, and the effect significantly increased with the coexistence of QA. Oppositely, IME suppressed the Zn and Ni depositions at the Zn partial current density of 100–300 A·m^{-2} and Ni partial current density of 10–20 A·m^{-2}, respectively, where the charge-transfer process became the rate-determining step (Figs. 2 and 3).

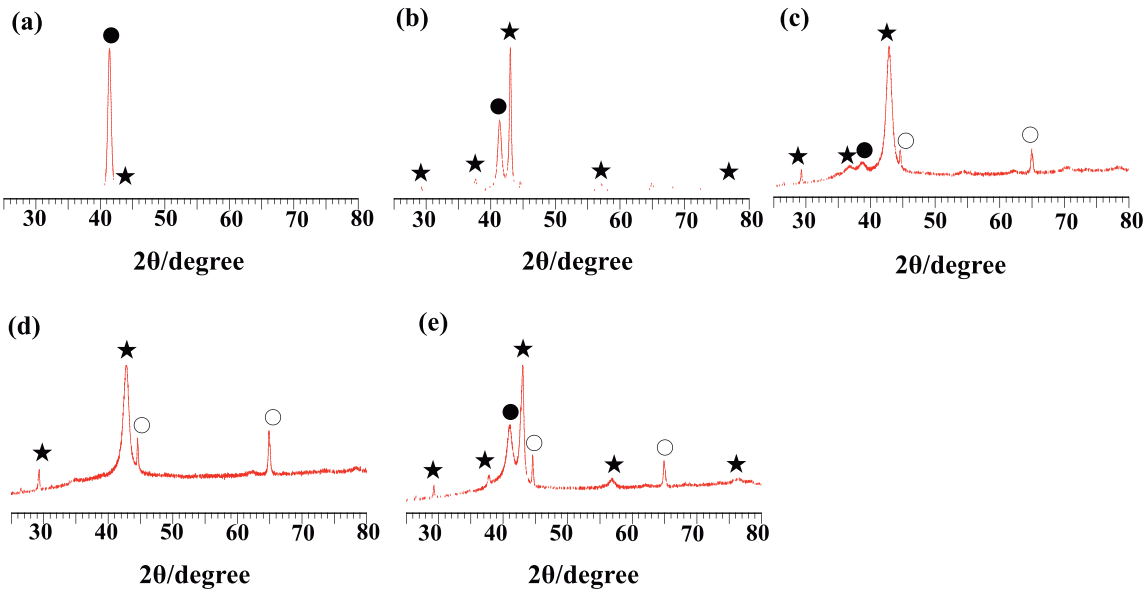

Fig. 11. X-ray diffraction patterns of the Zn–Ni alloy films deposited at 2 000 A·m^{-2} from the (a) brightener-free, (b) QA, (c) PQ, (d) PQ + QA, and (e) IME solutions. (○ Fe PDF # 65-4899, ● Zn[η] PDF # 87-0713, and ★ Ni_2Zn_{11}[γ] PDF # 65-5310) (Online version in color.)

Table 3. Summary of the effect of brighteners on the deposition behavior of the Zn–Ni alloy and its morphology.

	QA	PQ	PQ+QA	IME
Suppression effect	Charge transfer	Diffusion of ions	Diffusion of ions	Charge transfer
Transition C.D.	Decrease	Decrease	Decrease	Decrease
i_{Lim} of Zn	Not affected	Decrease	Decrease	Not affected
Ni% in deposit				
at C.D.<1 000 A·m^{-2}	Not affected	Decrease	Decrease	Decrease
at C.D.>1 000 A·m^{-2}	Not affected	Increase	Increase	Decrease
Current Efficiency				
at C.D.<1 000 A·m^{-2}	Not affected	Decrease	Decrease	Significantly decrease
at C.D.>1 000 A·m^{-2}	Increase	Significantly decrease	Significantly decrease	Decrease
Morphology at 2 000 A·m^{-2}	Coarsening	Smooth	Significantly smooth	Smooth

Thus, IME exerted a suppression effect on the charge-transfer process of the Zn–Ni alloy deposition. The effect of brighteners on the transition current density at which the deposition behavior shifted from normal to anomalous, the current efficiency of alloy deposition, and the composition, and morphology of the deposited films varied with the kind of brightener. Next, we discuss the factors for the low-current-density range (normal-type codeposition region at a potential nobler than E_{Zn}^{eq}), middle-current-density range (anomalous-type codeposition and charge-transfer rate-determining region at a potential less noble than E_{Zn}^{eq}), and high-current-density range (ion diffusion rate-determining region at a potential less noble than E_{Zn}^{eq}).

4.1. Effect of Brighteners on the Deposition Behavior of Zn–Ni Alloys

4.1.1. Low-current-density Region (Normal-type Codeposition at a Potential Region Nobler than E_{Zn}^{eq})

The transition current density of the Zn–Ni alloy deposition in this study was in the range of 50–100 $A \cdot m^{-2}$ without brighteners, whereas it was 20–50 $A \cdot m^{-2}$ with brighteners, regardless of the kind, showing a significant decrease in transition current density with brighteners (Fig. 6(a)). The transition current density of Zn–Ni alloy deposition is reported to decrease with the suppression of hydrogen evolution.[39–42] It is reported that the reduction reaction of H^+ proceeds through a multistep reaction via the adsorption of intermediate H_{ad}, and the adsorption site for H_{ad} is limited.[39–42] The formation of $Zn(OH)_2$ on the surface may suppress the hydrogen evolution reaction. It is also reported that IME added into solutions as a brightener suppresses the hydrogen evolution and decreases the transition current density.[21–26]

At a potential nobler than E_{Zn}^{eq}, hydrogen evolution was suppressed with the addition of PQ and PQ + QA (Fig. 4). Considering that the adsorption site for H atoms was limited, PQ and PQ + QA, as well as $Zn(OH)_2$ and IME, appeared to suppress the hydrogen evolution. During the Zn–Ni alloy deposition, PQ and PQ + QA suppressed the hydrogen evolution, resulting in a decrease in transition current density. However, although QA hardly suppressed the hydrogen evolution at a potential nobler than E_{Zn}^{eq} (Fig. 4), it decreased the transition current density, along with PQ, and IME. Although the degree of the suppression effect on the hydrogen evolution differed according to the kind of brightener, the transition current density was almost the same in all the solutions containing brighteners (Fig. 6(a)). The reason is unknown.

As shown in Fig. 2, Zn was significantly deposited even at approximately −0.9 V, which was nobler than its equilibrium potential in solutions without brighteners and containing QA, showing the apparent underpotential codeposition of Zn. The underpotential codeposition of Zn during Zn–Ni alloy deposition reportedly occurs because of the formation of a stable intermetallic compound, Ni_5Zn_{21}, by deposition, considerably reducing the activity coefficient of Zn in the deposited films.[42–45] Therefore, Ni codeposition is essential for the occurrence of Zn underpotential codeposition. Here, Zn underpotential codeposition appeared to occur because Ni was significantly deposited even at approximately −0.9 V, which was nobler than E_{Zn}^{eq} in solutions without brighteners and containing QA.

4.1.2. Middle-current-density Range (Anomalous-type Codeposition and Charge Transfer Rate-determining Region at a Potential Less Noble than E_{Zn}^{eq})

Regarding the effect of brighteners on the current efficiency of Zn–Ni alloy deposition, PQ and IME suppressed the depositions of Zn and Ni (Figs. 2–3), resulting in a decrease in current efficiency in the anomalous-type codeposition region (Fig. 5(a)). At a Zn partial current density below 300 $A \cdot m^{-2}$, *i.e.*, in the charge-transfer rate-determining region of Zn deposition, all the brighteners suppressed the Zn deposition, and the suppression effect was the highest with IME (Fig. 2). In the charge-transfer rate-determining region (total current density of 50–500 $A \cdot m^{-2}$), the current efficiency decreased the most with IME (Figs. 5(a)–5(b)), which was attributed to the highest suppression effect of IME on the Zn deposition.

Regarding the effect of brighteners on the composition of the deposited films, PQ and PQ + QA decreased the Ni content in the deposited films at 100–500 $A \cdot m^{-2}$, showing that Ni deposition was more intensely suppressed. IME as a brightener is reported to decrease the Ni content in films.[21–26] Assuming that the adsorption sites of intermediate $NiOH_{ad}$ were restricted during the Ni deposition, the adsorption sites of $NiOH_{ad}$ were blocked with IME, and Ni deposition was more intensely suppressed.[21–26] PQ and PQ + QA appeared to change the Ni content through the same mechanism as IME.

4.1.3. High-current-density Range (Ion Diffusion Rate-determining Region at a Potential Less Noble than E_{Zn}^{eq})

At a high Zn partial current density above 300 $A \cdot m^{-2}$, Zn deposition proceeded under the condition of the rate-determining step of ZnO_2^{2-} diffusion without brighteners, and the polarization effect of IME and QA on the Zn deposition was hardly observed in this region (Fig. 2). This was attributed to IME and QA having no suppression effect on the ZnO_2^{2-} diffusion. Contrarily, with PQ, the Zn deposition reached the diffusion-limiting current density at a Zn partial current density of approximately 200 $A \cdot m^{-2}$ (Fig. 2), indicating that PQ suppressed the ZnO_2^{2-} diffusion. With QA + PQ, the diffusion-limiting current density of Zn further decreased, indicating the synergistic suppression effect of PQ + QA on the ZnO_2^{2-} diffusion. The effect of brighteners on the Ni deposition was practically identical to that on the Zn deposition (Fig. 3). With PQ and PQ + QA, the Zn and Ni depositions easily reached the diffusion rate-determining step of ZnO_2^{2-} and the Ni ions, respectively (Figs. 2–3), further decreasing the current efficiency of the Zn–Ni alloy deposition at a high current density above 1 000 $A \cdot m^{-2}$ (Fig. 5). At a potential less noble than E_{Zn}^{eq}, hydrogen evolution was suppressed with QA (Fig. 4). The current efficiency was higher with QA than without brighteners in the middle- and high-current-density region of 200–2 000 $A \cdot m^{-2}$ (Fig. 5(a)), which appeared to be due to the suppression effect of QA on the hydrogen evolution.

In solutions containing PQ and PQ + QA, the characteristic behavior of the Ni content in the deposited films increasing as the current density increased above 1 000 $A \cdot m^{-2}$ was

observed (Fig. 6(b)). This was attributed to the fact that Zn, which was preferentially deposited over Ni, previously reached the diffusion-limiting current density of ZnO_2^{2-}, and Ni deposition had not yet reached the diffusion-limiting current density (Figs. 2–3), thereby increasing the Ni content of the deposited films with increasing current density. PQ had a suppression effect on the diffusion of ions in the solution; therefore, the characteristic behavior of the Ni content in deposited films increasing with current density was observed. The behavior of the diffusion of ZnO_2^{2-} being suppressed with PQ and PQ + QA was identical to that reported during Zn deposition from zincate solution,[27–30] and the same trend was observed during Zn–Ni alloy deposition. The factor of the synergistic suppression effect of PQ and QA on the diffusion of ZnO_2^{2-} has not been reported and is unknown.

PQ is a straight-chain polymer, and QA is a single quaternary ammonium salt. High-molecular-weight PQ has many adsorption sites and appears to adsorb on large areas of the cathode; contrarily, QA is a low-molecular-weight compound and is expected to adsorb on limited areas. Therefore, QA appeared to adsorb at the gaps between PQ, thereby potentially increasing the coverage of the brightener. Assuming that the coverage of the brightener increased, *i.e.*, the concentration of the brightener increased on the cathode, the viscosity of the solution around the cathode layer including the diffusion layer increased. Thus, the diffusion of ions in the diffusion layer can be said to have been suppressed.

4.2. Effect of Brighteners on the Microstructure of the Deposited Zn–Ni Alloy Films

At the diffusion-limiting current density, deposited films are generally reported to become granular or dendrite crystals.[46] However, in the solution containing PQ + QA in this study, the deposited films exhibited a smooth surface despite being deposited at the diffusion-limiting current density (2 000 $A \cdot m^{-2}$) of ZnO_2^{2-} (Fig. 10). PQ + QA suppressed the diffusions of ZnO_2^{2-} and Ni ions in addition to the charge-transfer process of the alloy deposition (Figs. 2–3). Thus, the crystal growth of the deposited films was suppressed, and the nucleation rate relatively increased, resulting in fine crystals. When the IME that suppresses the charge-transfer process was added, the surface of the films obtained at 2 000 $A \cdot m^{-2}$ became smoother than that without brighteners (Fig. 10), but the smoothness was less than that with PQ + QA. The suppression effect on the diffusion of ions in the solution appeared to have contributed to the improvement in the smoothness of deposited films.

Regarding the phase structure of the deposited films, with the addition of brighteners, the γ-phase was easily formed regardless of the Ni content in the deposited films (Figs. 9–11). When PQ and IME that increase the overpotential for deposition were added, the γ-phase was formed. According to the binary equilibrium diagram of the Zn–Ni system,[47] the stable region of the γ-phase at room temperature existed at the Ni content of 12.8–16.5 mass%. The films deposited at 200 $A \cdot m^{-2}$ from the solutions containing PQ and IME comprised the γ-phase regardless of the Ni content of 7.1 and 7.8 mass%, showing a different phase from that expected from the equilibrium diagram. The reason why the deposited films comprised the γ-phase only, regardless of the Ni content lower than that of the stable γ-phase region, was that the Zn formed a solid solution with the γ-phase, but the details are unknown. During electrodeposition, an increase in the overpotential for crystallization, *i.e.*, the suppression of the crystallization process is reported to produce films of the nonequilibrium phase (high-temperature phase), similar to the rapid quenching alloy because the reduced adatoms are crystallized in a supersaturation state.[48] The brightener is reported to suppress the crystallization process in addition to the charge-transfer process.[49] Here, since the crystallization overpotential for deposition increased with brighteners, the reduced adatoms of Zn and Ni (Zn_{ad} and Ni_{ad}) were supersaturated. Thus, the γ-phase appeared to be formed in a Ni content region different from that expected from the equilibrium diagram.

5. Conclusions

The deposition behavior of Zn–Ni alloys in zincate solution (ZnO (0.15 $mol \cdot dm^{-3}$), $NiSO_4 \cdot 6H_2O$ (0.016 $mol \cdot dm^{-3}$), $N(CH_2CH_2OH)_3$ (0.34 $mol \cdot dm^{-3}$), NaOH (2.5 $mol \cdot dm^{-3}$), and 303 K) containing various brighteners and their microstructure were investigated. The transition current density at which the deposition behavior shifted from normal to anomalous decreased with the addition of brighteners. Although the suppression effect of brighteners on the hydrogen evolution differed depending on the kind of brightener, the transition current density was almost the same in all the solutions containing brighteners. The current efficiency for alloy deposition significantly decreased with the addition of brighteners, which had a suppression effect on the Zn deposition. Considering that the brighteners suppressed the Ni deposition more than the Zn deposition, the Ni content in the deposited films decreased with the addition of brighteners. When the brightener of a straight-chain polymer composed of a quaternary ammonium cation (PQ), which can suppress the diffusion of ZnO_2^{2-} and Ni ions in solution, was added, the characteristic behavior of the Ni content in the deposited films increasing with increasing current density at a high current density was observed. This was attributed to the fact that Zn, which was preferentially deposited over Ni earlier, reached the diffusion limitation of ZnO_2^{2-}, and the Ni deposition did not reach the diffusion-limiting current density. When both PQ and a quaternary ammonium salt with a benzene ring were added to the solution, the films obtained at the diffusion-limiting current density of ZnO_2^{2-} exhibited smooth surfaces comprising fine crystals. With the addition of brighteners to increase the deposition overpotential, the γ-phase of the deposited films was easily formed regardless of the Ni content in the deposited films.

REFERENCES

1) R. Ramanauskas: *Appl. Surf. Sci.*, **153** (1999), 53. https://doi.org/10.1016/S0169-4332(99)00334-7
2) Z. Feng, Q. Li, J. Zhang, P. Yang, H. Song and M. An: *Surf. Coat. Technol.*, **270** (2015), 47. https://doi.org/10.1016/j.surfcoat.2015.03.020
3) S. H. Mosavat, M. H. Shariat and M. E. Bahrololoom: *Corros. Sci.*, **59** (2012), 81. https://doi.org/10.1016/j.corsci.2012.02.012
4) O. Girčienė, L. Gudavičiūtė, R. Juškėnas and R. Ramanauskas: *Surf. Coat. Technol.*, **203** (2009), 3072. https://doi.org/10.1016/j.surfcoat.2009.03.030
5) Z. Feng, L. Ren, J. Zhang, P. Yang and M. An: *RSC Adv.*, **6** (2016),

88469. https://doi.org/10.1039/C6RA18476F
6) A. El Hajjami, M. P. Gigandet, M. De Petris-Wery, J. C. Catonne, J. J. Duprat, L. Thiery, F. Raulin, N. Pommier, B. Starck and P. Remy: *Appl. Surf. Sci.*, **254** (2007), 480. https://doi.org/10.1016/j.apsusc.2007.06.016
7) M. Yano, H. Fukushima, H. Nakano and T. Akiyama: *Tetsu-to-Hagané*, **86** (2000), 176 (in Japanese). https://doi.org/10.2355/tetsutohagane1955.86.3_176
8) T. Fujigaya: Mekki Gizyutsu Gaido (Electroplating, Chemical Plating and Engineering Guide), the Japan Suppliers Association of Plating Materials, Tokyo, (2004), 143 (in Japanese).
9) M. Kawasaki and H. Enomoto: Mekki Kyohon (Textbook for Plating), The Nikkan Kogyo Shimbun, Tokyo, (1986), 108 (in Japanese).
10) A. Brenner: Electrodeposition of Alloys, Vol. 2, Academic Press, New York, (1963), 194.
11) H. Fukushima, T. Akiyama, J.-h. Lee, M. Yamaguchi and K. Higashi: *J. Met. Finish. Soc. Jpn.*, **33** (1982), 574 (in Japanese). https://doi.org/10.4139/sfj1950.33.574
12) H. Fukushima, T. Akiyama, M. Yano, T. Ishikawa and R. Kammel: *ISIJ Int.*, **33** (1993), 1009. https://doi.org/10.2355/isijinternational.33.1009
13) H. Nakano, S. Kobayashi, T. Akiyama, T. Tsuru and H. Fukushima: *Tetsu-to-Hagané*, **89** (2003), 64 (in Japanese). https://doi.org/10.2355/tetsutohagane1955.89.1_64
14) H. Nakano, M. Matsuno, S. Oue, M. Yano, S. Kobayashi and H. Fukushima: *J. Jpn. Inst. Met.*, **69** (2005), 548 (in Japanese). https://doi.org/10.2320/jinstmet.69.548
15) M. G. Hosseini, H. Ashassi-Sorkhabi and H. A. Y. Ghiasvand: *Surf. Coat. Technol.*, **202** (2008), 2897. https://doi.org/10.1016/j.surfcoat.2007.10.022
16) L. S. Tsybulskaya, T. V. Gaevskaya, O. G. Purovskaya and T. V. Byk: *Surf. Coat. Technol.*, **203** (2008), 234. https://doi.org/10.1016/j.surfcoat.2008.08.067
17) G. Y. Li, J. S. Lian, L. Y. Niu and Z. H. Jiang: *Surf. Coat. Technol.*, **191** (2005), 59. https://doi.org/10.1016/j.surfcoat.2004.04.062
18) N. R. Short, S. Zhou and J. K. Dennis: *Surf. Coat. Technol.*, **79** (1996), 218. https://doi.org/10.1016/0257-8972(95)02428-X
19) C. Müller, M. Sarret and M. Benballa: *J. Electroanal. Chem.*, **519** (2002), 85. https://doi.org/10.1016/S0022-0728(01)00725-2
20) H. Y. Lee and S. G. Kim: *Surf. Coat. Technol.*, **135** (2000), 69. https://doi.org/10.1016/S0257-8972(00)00731-3
21) S. H. Bae, S. Oue, I. Son and H. Nakano: *Tetsu-to-Hagané*, **107** (2021), 229 (in Japanese). https://doi.org/10.2355/tetsutohagane.TETSU-2020-108
22) S. H. Bae, S. Oue, I. Son and H. Nakano: *ISIJ Int.*, **61** (2021), 2256. https://doi.org/10.2355/isijinternational.ISIJINT-2021-080
23) S. H. Bae, S. Oue, Y.-k. Taninouchi, I. Son and H. Nakano: *Tetsu-to-Hagané*, **108** (2022), 120 (in Japanese). https://doi.org/10.2355/tetsutohagane.TETSU-2021-092
24) S. H. Bae, S. Oue, Y.-k. Taninouchi, I. Son and H. Nakano: *ISIJ Int.*, **62** (2022), 1522. https://doi.org/10.2355/isijinternational.ISIJINT-2022-076
25) S. H. Bae, S. Oue, Y.-k. Taninouchi, I. Son and H. Nakano: *Tetsu-to-Hagané*, **108** (2022), 268 (in Japanese). https://doi.org/10.2355/tetsutohagane.TETSU-2021-105
26) S. H. Bae, S. Oue, Y.-k. Taninouchi, I. Son and H. Nakano: *ISIJ Int.*, **62** (2022), 1918. https://doi.org/10.2355/isijinternational.ISIJINT-2022-160
27) K. Fukumoto, S. Oue, Y. Kikuchi, S. Akamatsu, T. Takasu and H. Nakano: *J. Jpn. Inst. Met.*, **83** (2019), 399 (in Japanese). https://doi.org/10.2320/jinstmet.J2019027
28) K. Fukumoto, S. Oue, Y. Kikuchi, S. Akamatsu, T. Takasu and H. Nakano: *Mater. Trans.*, **61** (2020), 497. https://doi.org/10.2320/matertrans.MT-M2019316
29) K. Fukumoto, S. Oue, T. Niwa, Y. Kikuchi, S. Akamatsu and H. Nakano: *Mater. Trans.*, **62** (2021), 807. https://doi.org/10.2320/matertrans.MT-M2021027
30) K. Fukumoto, S. Oue, T. Niwa, Y. Kikuchi, S. Akamatsu and H. Nakano: *J. Jpn. Inst. Met.*, **85** (2021), 59 (in Japanese). https://doi.org/10.2320/jinstmet.J2020043
31) H. Nezu, S. Fujii, N. Kaneko and N. Ofuchi: *J. Met. Finish. Soc. Jpn.*, **32** (1981), 17 (in Japanese). https://doi.org/10.4139/sfj1950.32.17
32) S. Konishi, S. Eguchi, N. Ozeki and M. Uesugi: *J. Met. Finish. Soc. Jpn.*, **20** (1969), 263 (in Japanese). https://doi.org/10.4139/sfj1950.20.263
33) M. Pourbaix: Atlas of Electrochemical Equilibria in Aqueous Solutions, Pergamon Press, New York, (1966), 406.
34) D. D. Perrin: Stability Constants of Metal-ion Complexes, Part B: Organic Ligands, Pergamon Press, Oxford, UK, (1979), 466.
35) T. Akiyama, H. Fukushima and K. Higashi: *Tetsu-to-Hagané*, **72** (1986), 918 (in Japanese). https://doi.org/10.2355/tetsutohagane1955.72.8_918
36) H. Nakano, S. Shibata, S. Arakawa, S. Oue and S. Kobayashi: *ISIJ Int.*, **53** (2013), 1858. https://doi.org/10.2355/isijinternational.53.1858
37) H. Nakano, S. Shibata, S. Arakawa, S. Oue and S. Kobayashi: *Tetsu-to-Hagané*, **99** (2013), 346 (in Japanese). https://doi.org/10.2355/tetsutohagane.99.346
38) M. Sagiyama, M. Kawabe and T. Watanabe: *Tetsu-to-Hagané*, **76** (1990), 1301 (in Japanese). https://doi.org/10.2355/tetsutohagane1955.76.8_1301
39) H. Fukushima and H. Nakano: *J. Surf. Sci. Soc. Jpn.*, **22** (2001), 107 (in Japanese). https://doi.org/10.1380/jsssj.22.107
40) H. Nakano, T. Ohgai, H. Fukushima, T. Akiyama and R. Kammel: *Metall*, **55** (2001), 676.
41) H. Fukushima, T. Akiyama and K. Kiyotani: *Shigen-to-Sozai*, **109** (1993), 861 (in Japanese). https://doi.org/10.2473/shigentosozai.109.861
42) H. Nakano, S. Arakawa, Y. Takada, S. Oue and S. Kobayashi: *Mater. Trans.*, **53** (2012), 1946. https://doi.org/10.2320/matertrans.M2012241
43) H. Nakano, S. Arakawa, Y. Takada, S. Oue and S. Kobayashi: *J. Jpn. Inst. Met.*, **76** (2012), 443 (in Japanese). https://doi.org/10.2320/jinstmet.76.443
44) H. Nakano, S. Arakawa, S. Oue and S. Kobayashi: *Tetsu-to-Hagané*, **99** (2013), 425 (in Japanese). https://doi.org/10.2355/tetsutohagane.99.425
45) H. Nakano, S. Arakawa, S. Oue and S. Kobayashi: *ISIJ Int.*, **53** (2013), 1864. https://doi.org/10.2355/isijinternational.53.1864
46) R. Winand: *J. Appl. Electrochem.*, **21** (1991), 377. https://doi.org/10.1007/BF01024572
47) M. Hansen: Constitution of Binary Alloys, McGraw-Hill, New York, (1958), 1060.
48) S. Haruyama: Hyomen Gizyutsusya no tameno Denkikagaku (Electrochemistry for Surface Engineer), Maruzen, Tokyo, (2005), 155 (in Japanese).
49) S. Haruyama: Hyomen Gizyutsusya no tameno Denkikagaku (Electrochemistry for Surface Engineer), Maruzen, Tokyo, (2005), 178 (in Japanese).